Why is adiabatic compressed air energy storage yet to become a viable energy storage option?

Barbour, Edward R.; Pottie, Daniel L.; Eames, Philip

DOI:
10.1016/j.isci.2021.102440

Document Version
Publisher's PDF, also known as Version of record

Citation for published version (Harvard):
Barbour, ER, Pottie, DL & Eames, P 2021, 'Why is adiabatic compressed air energy storage yet to become a viable energy storage option?', *iScience*, vol. 24, no. 5, 102440. https://doi.org/10.1016/j.isci.2021.102440

iScience

CellPress
OPEN ACCESS

Perspective

Why is adiabatic compressed air energy storage yet to become a viable energy storage option?

Edward R. Barbour,[1,*] Daniel L. Pottie,[1] and Philip Eames[1]

SUMMARY

Recent theoretical studies have predicted that adiabatic compressed air energy storage (ACAES) can be an effective energy storage option in the future. However, major experimental projects and commercial ventures have so far failed to yield any viable prototypes. Here we explore the underlying reasons behind this failure. By developing an analytical idealized model of a typical ACAES design, we derive a design-dependent efficiency limit for a system with hypothetical, perfect components. This previously overlooked limit, equal to 93.6% under continuous cycling for a typical design, arises from irreversibility associated with the transient pressure in the system. Although the exact value is design dependent, the methodology we present for finding the limit is applicable for a wide range of designs. Turning to real systems, the limit alone does not fully explain the failure of practical ACAES research. However, reviewing the available evidence alongside our analytical model, we reason that underestimation of the system complexity, difficulty with the integration of off-the-shelf components, and a number of misleading performance claims are the primary reasons hindering ACAES development.

INTRODUCTION

Adiabatic compressed air energy storage (ACAES) is a concept for thermo-mechanical energy storage with the potential to offer low-cost, large-scale, and fossil-fuel-free operation. The operation is described simplistically as follows. To charge the system, work is used to compress atmospheric air in compressors (Figure 1 point (1)), generating heat in the process. The heat at the compressor outlets is removed from the air via heat exchangers (HEX) and stored in separate thermal energy stores (TES) (Figure 1 point (2)), whereas the cool compressed air is stored in a high-pressure (HP) air store (Figure 1 point (3)). To discharge the system, the cool compressed air is recombined with the heat from the TES to generate hot, high-pressure air (Figure 1 point (4)), which is expanded through turbines to generate work (Figure 1 point (5)). Figure 1 depicts the process.

Despite having a very similar name, ACAES is distinct from current compressed air energy storage (CAES) plants, which are diabatic. Two utility-scale CAES plants—Huntorf, DE (321*MW*) and MacIntosh, USA (110*MW*)—have existed since 1978 and 1991 respectively, using salt caverns as underground storage (Crotogino et al., 2001; Hounslow et al., 1998). These systems also charge by using work to compress atmospheric air, generating heat in the process; however, the heat is wasted and exergy is stored only in the cool pressurized air. When the system is discharged, this air is heated using fossil fuel (typically natural gas) and is used to drive a turbine. Hence, this system arguably has more similarity with gas turbine technology than a pure energy storage plant. Rather, the major difference between CAES and a gas turbine is the temporal decoupling of the compressor and turbine operation, which requires the storage of compressed air. As such, CAES has significant associated emissions (these are estimated at $228 g_{CO_2}/kWh$ when charged with wind energy—60% of the emissions reported for gas turbines [Mason and Archer, 2012]) and cannot be considered solely as an electricity storage system, such as batteries or pumped hydroelectric storage.

As a result of the shortcomings of CAES and due to the appeal of a purely thermo-mechanical energy storage system, with no reliance on either fossil fuel or rare materials, much recent research has focused on

[1]Centre for Renewable Energy Systems Technology, Loughborough University, Loughborough, UK

*Correspondence: e.r.barbour@lboro.ac.uk

https://doi.org/10.1016/j.isci.2021.102440

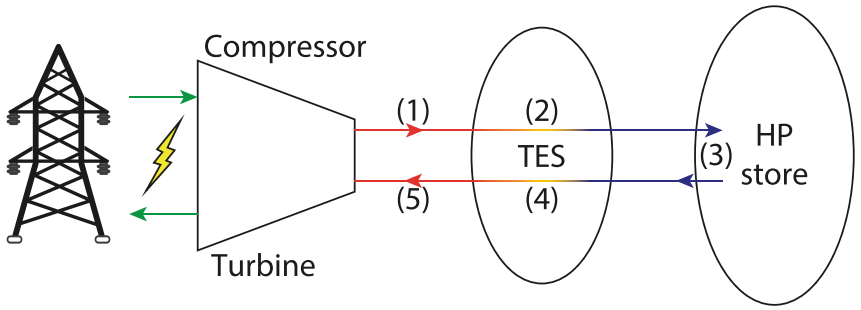

Figure 1. ACAES system definition
Thermo-mechanical processes that define ACAES.

ACAES. Most of these studies use numerical thermodynamic models (Grazzini and Milazzo, 2008; Barbour et al., 2015; Sciacovelli et al., 2017) or (generally small-scale) experimental work augmented with numerical aspects to predict the electrical-to-electrical efficiency, typically in the range 50%–75% (Grazzini and Milazzo, 2008; Barbour et al., 2015; Sciacovelli et al., 2017; Szablowski et al., 2017; Peng et al., 2016). The exact value predicted depends on the assumed performance of the constituent components as well as the precise system configuration, with lower estimates typically taking a more pessimistic view of component performance. However, the thermodynamic performance limits of ACAES are under-explored and it should be noted that no prototype system has attained the predicted performance.

Here, we demonstrate here that the efficiency limit of typical designs is considerably lower than 100%—indeed, for the design illustrated in Figure 2 we find a limit of 93.6%. Although the exact limit is specific to the design proposed, our methodology can be applied to designs with differing numbers of stages and the loss mechanisms are the same. The limit arises due to exergy destruction as heat at different temperatures is mixed in the system and the exhaust, as well as throttling losses. This unavoidable penalty has been overlooked by previous research, and although by itself it does not explain the failure of ACAES development to yield a viable design, it highlights the target component operation for ACAES to reach maximum performance. Comparing this operation to that available from conventional components and analyzing the available literature in the scientific and public domains, we postulate that three additional issues have hindered ACAES development. These are as follows. (1) Underestimation of the real process complexity and the misconception that the system can be built with *off-the-shelf* compressors, turbines, and heat exchangers. (2) Misleading efficiency claims from early-stage commercial projects, often repeated in academic review articles, and unrealistic assumptions in previous modeling work, which are rarely challenged. (3) A combination of the reasons (1) and (2) leading to over-ambitious development in commercial ventures, where any lessons learned are hidden, in turn stifling much-needed transparent experimental projects. Furthermore, the high investment costs of prototype ACAES systems are a major challenge, although this is a common hurdle across thermo-mechanical energy storage development.

We therefore recommend the following three actions to improve the prospects of ACAES as a potential large-scale energy storage option. (1) Further transparent experimental work on ACAES in universities, which is crucial for understanding detailed system performance. (2) Where commercial projects are funded with majority public money, a minimum threshold of documentation should be stipulated, which, in the event of project termination, must include the reasons for failure to achieve the stated aims. (3) High-quality research and funding should not be influenced by hearsay or unverifiable performance claims; in particular, opaque performance claims with a lack of documentation for commercial sensitivity reasons should not influence academic research until verified.

RESULTS

Thermodynamic limits

We now discuss the efficiency limits of the typical ACAES design as shown in Figure 2. The purpose is to reveal both the theoretical efficiency limit and the corresponding operation of the system components. Accordingly, we consider the limit in which all components are ideal and reversible (except for the throttle valve, which is ideal but not reversible) and we treat air as a dry, ideal gas with constant specific heats c_p and c_v. The HP air store has a constant volume (i.e., isochoric), and during the charging period, air is added at

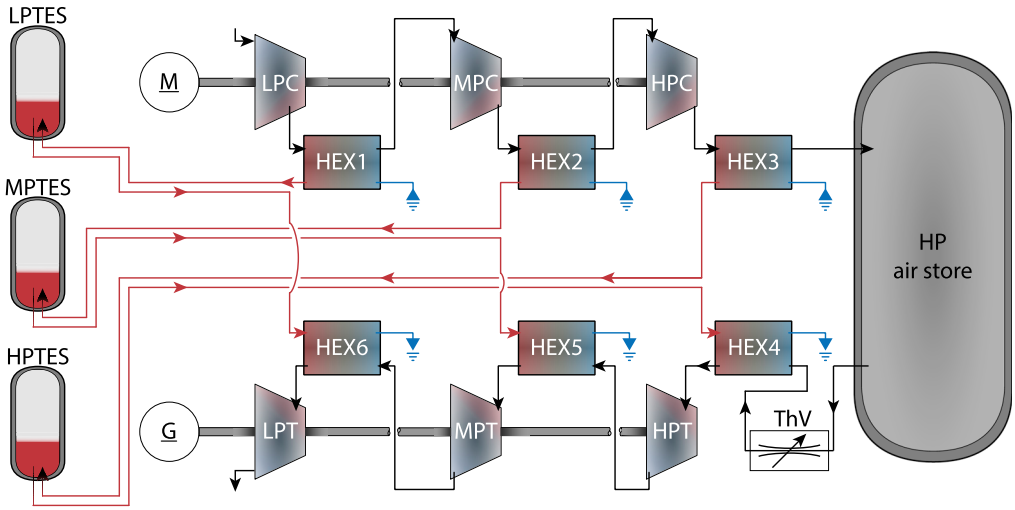

HEX	Heat exchanger				
M	Motor	G	Generator	ThV	Throttle valve
Low pressure		*Medium pressure*		*High pressure*	
LPC	Compressor	MPC	Compressor	HPC	Compressor
LPT	Turbine	MPT	Turbine	HPT	Turbine
LPTES	Thermal Energy Storage	MPTES	Thermal Energy Storage	HPTES	Thermal Energy Storage

Figure 2. Case study ACAES system

A schematic of an ACAES system that belies the complexity. Purely adiabatic compressors with variable compressor ratios must operate efficiently. Cooling stages should have minimal pressure drop and maximum effectiveness. Heat and mixing losses in the TES and HP store should be minimized. Steady flow should be maintained during expansion, and heating stages should exactly reverse the cooling stages. Effective integration between components is crucial and control must be maintained under all conditions. For this system and assuming hypothetical perfectly ideal components we find that 6.4% of the input work is unrecoverable.

ambient temperature because perfect counter-current exchangers are assumed. We treat the HP air store as adiabatic during the charge and discharge processes, so the air compression during charging leads to a significant temperature increase. This is justified by the need for high tensile stress tolerance in the HP store for operation and safety, meaning a store with a large surface-area-to-volume ratio will not be practical. We also note that real CAES systems experience significant temperature rise during charging and temperature drop during discharging (Crotogino et al., 2001; Raju and Khaitan, 2012) and similar temperature behaviors are experienced in experiments on ACAES systems (Geissbühler et al., 2018; Wang et al., 2016a). During the idle periods (between charging/discharging and discharging/charging) we consider two limiting cases, an adiabatic store (denoted AD) in which no heat is exchanged with the environment and a store that undergoes temperature recovery (denoted TR) to the ambient temperature. Under these assumptions, the charging work is given by Equation 1 (see methods).

$$W^{chg} = N\frac{V^{st}c_p p_i^{chg}}{R\gamma}\left\{\frac{1}{\frac{\gamma-1}{N\gamma}+1}\left[\frac{p_f^{chg}}{p_i^{chg}}\left(\frac{p_f^{chg}}{p^0}\right)^{\frac{\gamma-1}{N\gamma}} - \left(\frac{p_i^{chg}}{p^0}\right)^{\frac{\gamma-1}{N\gamma}}\right] + 1 - \frac{p_f^{chg}}{p_i^{chg}}\right\} \quad \text{(Equation 1)}$$

In Equation 1, pressures p_i^{chg} and p_f^{chg} are the initial and final HP store pressures, respectively, during the charge and N is the number of compression stages (each stage has equal compression ratio). The parameter γ is the ratio of the specific heats at standard conditions and signifies compression along an isentropic reversible path. Equation 2 gives the temperature in the HP air store as a result of the air compression within (see methods).

$$T_f^{chg} = \frac{\gamma T^0}{\frac{p_i^{chg}}{p_f^{chg}}\left(\gamma\frac{T^0}{T_i^{chg}} - 1\right) + 1} \quad \text{(Equation 2)}$$

T_i^{chg} is the initial store temperature for the charging process, which is equal to the ambient for the first cycle. The compression work is stored as exergy partly in the HP air store and partly in the TES (Budt et al., 2016). Although there is a separate TES for each compression stage—because imperfect heat exchange leads to successive increases in compressor outlet temperature—with perfect heat exchange, the temperature of each TES is the same. The compressor outlet temperatures are variable and are a function of the instantaneous pressure ratio and the inlet air temperature. In the limit of perfect heat exchange and isentropic compression, the TES temperature is the average compressor outlet temperature, as expressed by Equation 3 (see methods).

$$T^{TES} = \frac{T^0 p_i^{chg}}{\left(\frac{\gamma-1}{N\gamma}+1\right)\left(p_f^{chg}-p_i^{chg}\right)}\left[\frac{p_f^{chg}}{p_i^{chg}}\left(\frac{p_f^{chg}}{p^0}\right)^{\frac{\gamma-1}{N\gamma}} - \left(\frac{p_i^{chg}}{p^0}\right)^{\frac{\gamma-1}{N\gamma}}\right] \quad \text{(Equation 3)}$$

This also provides the maximum reheat temperature available during discharge, assuming no TES cooling during the idle period. Hence the maximum recoverable work is:

$$W^{dis} = N\frac{c_p T^{TES} V^{st}}{R T_i^{dis}}\left(1-\left(\frac{p^{thr}}{p^0}\right)^{\frac{1-\gamma}{N\gamma}}\right)\left[p_i^{dis} - p^{thr}\left(\frac{p^{thr}}{p_i^{dis}}\right)^{\frac{1-\gamma}{\gamma}}\right] \quad \text{(Equation 4)}$$

In Equation 4, p_i^{dis} and T_i^{dis} are the initial discharge pressure and temperature of the store while the minimum pressure is the throttle pressure p^{thr}. The recovered work clearly depends on the throttle pressure, which regulates the pressure entering the turbines, allowing design-point operation. This increases their reliability and efficiency (Sciacovelli et al., 2017; Zhang et al., 2019; He et al., 2017) at the necessary cost of some exergy destruction due to the air entropy change through the throttle. The round trip efficiency of the system is given by:

$$\eta^{RT} = \frac{W^{dis}}{W^{chg}} \quad \text{(Equation 5)}$$

The implications of Equations 1, 2, 3, 4, and 5 are illustrated in Figure 3A. We take the base case for our typical system as a $1,000 m^3$ store with minimum pressure $4 MPa$, maximum pressure $7 MPa$, $N = 3$ compression and expansion stages, and air throttled to $4 MPa$ before expansion. These pressures limits are similar to the conditions at Huntorf and McIntosh and those assumed in previous studies (Sciacovelli et al., 2017; Zhang et al., 2019; He et al., 2017). With these assumptions we find an efficiency limit of 88.2% for the first cycle, which rises to 93.6% (as calculated by Equation 5) under continuous cycling for the adiabatic (AD) store (see Figure 3B). With continuous cycling we assume that the mass of air in the HP store remains constant between the end of the discharge of the previous cycle and start of the charge in the next. Hence in the AD case the pressure and temperature remain unchanged during the time between cycles, whereas in the TR case the pressure at the start of the next cycle is higher as the store temperature recovers to the ambient. We note that it takes approximately five cycles for the mass to stabilize for the TR case and 20 cycles for the AD case.

The results are summarized in Table 1. The exergy accounting for both systems is shown in Figure 3C, with the full analytic exergy accounting method described in supplemental information section S1 and summarized in Table S1 (the method is general for any number of stages). Although the efficiency limit of both systems (AD and TR) under continuous cycling is high, it must be emphasized that these are idealized limits. That is explicitly to say that they represent the *design maximum possible efficiency*, so 6.4% of the input exergy is unrecoverable even with perfectly ideal components in the AD case, rising to 7.5% for the TR case.

For the AD case, direct throttling losses are the largest loss, and the first cycle is also restricted by the large proportion of air that cannot be extracted from the store due to the discharge temperature drop (Figure 3D), leaving exergy remaining in the HP store and TES (Figure 3C). These effects combine to limit the first cycle efficiency to 88.2%. Once the mass has stabilized (Figures 3D and 3E), the efficiency rises to 93.6% and the throttling losses are dominant, with small mixing losses in the HP store, the TES, and exhaust streams. For the TR case, the first cycle efficiency is 69.9% due to the air mass that cannot be extracted due to the temperature drop. However, after five cycles the air mass added and extracted has stabilized and the initial storage pressure has increased to $4.57 MPa$, as can be seen in the difference between final temperature, pressure and mass added and extracted in Figures 3F and 3G, yielding an efficiency limit of 92.5%. Figure 3C shows that once stabilized throttling accounts for the majority of the exergy destruction in both the AD and TR systems. The throttling also increases downstream losses in the exhaust fluid streams; however, these are small in magnitude.

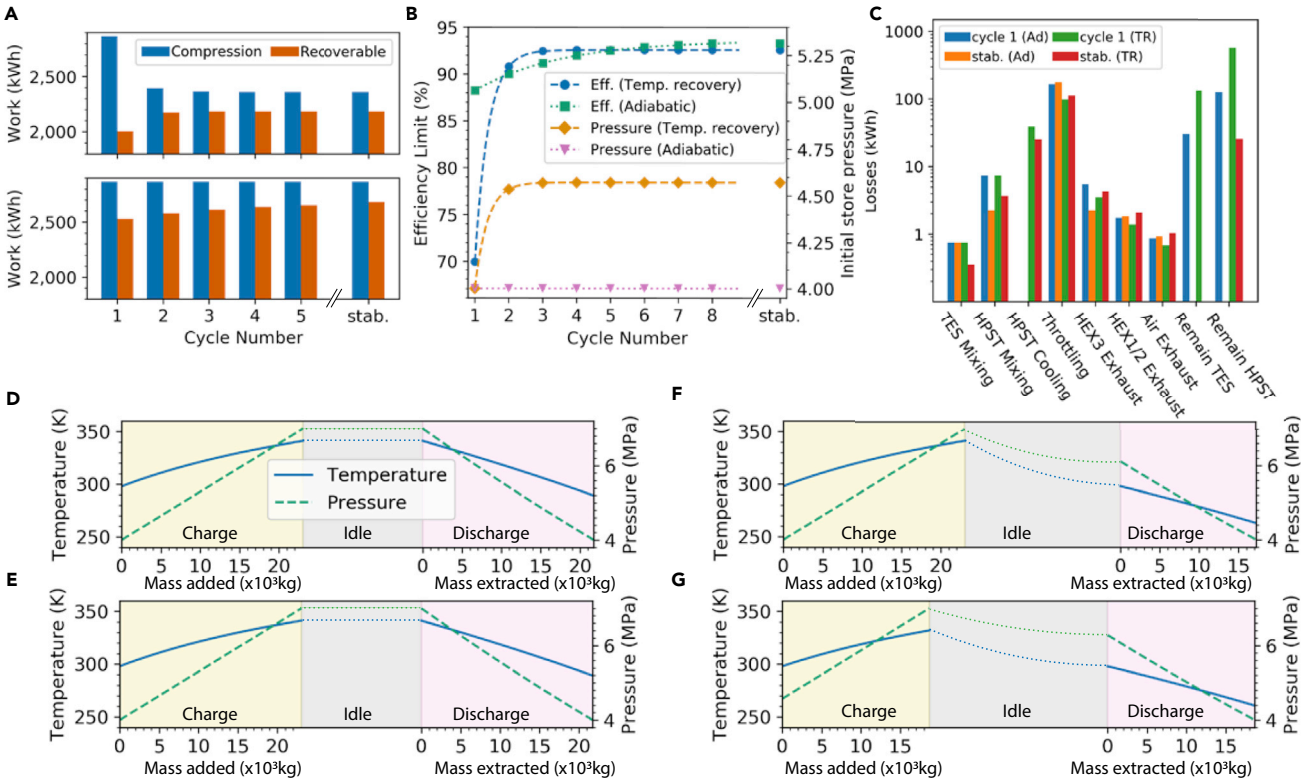

Figure 3. Summary of performance and results

Efficiency limits for the proposed ACAES system (1,000 m^3).

(A) Compression and recoverable work over five cycles and for a stabilized cycle (stab.).

(B) Efficiency limit and initial store pressure over 10 cycles.

(C) Exergy accounting for the adiabatic store (denoted AD) and temperature recovery (denoted TR) systems.

(D–G) Illustration of the pressure and temperature changes during the charging, idle, and discharge periods for (D) the first cycle with AD store, (E) a stabilized cycle with AD store, (F) the first cycle TR store, and (G) a stabilized cycle with TR store. The differences between (D) and (E) and (F) and (G) illustrate how the mass of air added/extracted from the HP store equalizes compared with the initial cycle. Temperature and pressure in the idle period are qualitatively illustrated.

The exact efficiency limit revealed is design-dependent (although it does not depend on the store volume), as is illustrated by the differences between the AD and TR cases. However, it is widely applicable given the similarity between the majority of designs proposed in available literature and Figure 2. Furthermore, our approach is general for any number of stages. Importantly, the analysis reveals the complexity of idealized ACAES, demonstrating that even with highly efficient components the losses associated with thermal mixing will quickly become non-negligible. In real systems, the store will not be completely adiabatic during charging/discharging and thermal conduction through the walls will influence the air temperature. This effect will become more relevant as the power-to-energy ratio of the system decreases, and previous work has shown that caverns with large discharge times can deviate significantly from the adiabatic assumption (Raju and Khaitan, 2012). However, these studies also showed that this difference is small for relatively short charge/discharge times, which is likely applicable for artificial air stores with low surface-area-to-volume ratio.

Table 1. Calculated efficiency limits for isochoric idealized ACAES

	HP store heat regime	
	Adiabatic (AD)	Temperature recovery (TR)
First cycle	88.2%	69.9%
Continuous cycling	93.6%	92.5%

Challenges for ACAES components

There is a common misconception that the majority of components in the ACAES system shown in Figure 2 can be acquired "*off-the-shelf.*" Indeed, engineers are very familiar with industrial compressors, turbines, and HEX, and for many applications these items can be ordered as standard. However, for use in ACAES there are many crucial differences between the constituent components and their counterparts developed for previous applications. We discuss challenges for ACAES compressors, HEX, and expanders and highlight how they differ from readily available components. The HP store also has design challenges; however, in its simplest form a pressure vessel with suitable tolerance could be used.

Compressors

In ACAES, the compressions should be adiabatic (i.e., isentropic and reversible), with all heat exchange taking place in the dedicated HEX that supplies the TES, otherwise the compression process will not follow a reversible path. In contrast, compressors for many other applications are designed to minimize the work input per unit production of high-pressure air, which typically involves simultaneous compression and cooling. This cooling of the compressor, while reducing the compression work, leads to additional irreversibility generation on top of the unavoidable frictional, leakage, and aerodynamic losses. The compressors in ACAES should also have high single-stage pressure ratios (>3) with high isentropic efficiency to achieve good energy density. These constraints make the use of axial compressors difficult because they are unable to reach higher pressure ratios without introducing sonic flow choke or having to design adequate convergent-divergent blade sections to achieve an efficient transonic transition. Moreover, the compressor operating principle causes the air flow to decelerate, creating an adverse pressure gradient, which can lead to stall and surge. This results in smaller allowable pressure ratios in compressors than axial turbines. These challenges are not only cost related, as more compression stages are required for the same pressure ratio, but also there are thermodynamic downsides arising from asymmetrical pressure distributions in charge/discharge. In contrast with axial machines, reciprocating compressors are able to reach the required pressure ratio without facing these issues, as the compression takes place on mostly stationary air. However, the mass flow capability of positive displacement machines is (relatively) smaller than axial, and ACAES charge requirements might lead to unpractical designs such as large piston diameters or several simultaneous chambers in parallel.

A further design challenge is that with isochoric air storage the compressors must function at high efficiency over a range of pressure ratios (Sciacovelli et al., 2017). This challenge is illustrated by recent studies with compressor models calibrated from experimental data, the results of which indicate that compressor performance deteriorates rapidly as the operation range increases (Chen et al., 2020; Ma et al., 2019). The range of pressure ratios encountered also necessitates that compressors operate with variable mass flow if constant power is to be achieved, which is further detrimental for performance (Sun et al., 2020). It is notable that poor compressor performance due to the range of pressure ratios encountered and unsteady mass flow rates is suggested as a primary reason for the low performance of prototype experimental ACAES systems (Wang et al., 2016a).

Heat exhangers

The HEX required for ACAES are also highly non-standard and, like the compressors, must operate with variable mass flow, which is a design challenge (Zhang et al., 2019). Here, HEX1 – 3 are compressor aftercoolers while HEX4 – 6 are turbine preheaters (see Figure 2). The compressor coolant should enter the TES as close as possible to the compressor outlet temperature, necessitating a HEX temperature cross, which will be challenging to design cost effectively. In typical compressor aftercooler designs, heat transfer is enhanced by increasing the available heat transfer area and the air-to-coolant temperature difference. The effect of the former is limited by manufacturing techniques, cost restriction, and footprint available. To achieve the latter, however, the coolant mass flow rate is set considerably higher than the required mass flow for a balanced HEX, reducing the coolant temperature rise to maintain the thermal gradient with the air. This greatly improves the heat exchanger effectiveness; however, it reduces the process reversibility. The requirement for both cooling (during charge) and later reheating (during discharge) demands high process reversibility. This introduces a natural trade-off because (1) compressors operate better when the aftercooler coolant flow rate increases well above the balanced requirements but (2) to guarantee proper turbine inlet temperature, the coolant flow rate must meet the balanced requirements for the HEX. Therefore, ACAES heat exchangers need considerably larger contact areas than conventional aftercoolers, and it is of paramount importance to ensure that this does not lead to exceedingly large pressure losses in all HEX stages. The need to balance the HEX at all times is also a control challenge (Shah and Sekulic, 2003).

In general for ACAES, the number of cooling and heating stages is a design choice, with more stages leading to lower compressor outlet and TES temperatures. However, there are practical limits on the number of compressors and HEX it is possible to link in series without introducing severe pressure losses. Therefore most designs opt for between two and four stages, which predicates high temperatures at the compressor outlets, rendering even pressurized liquid water an impractical coolant. Hence various thermal oils have been suggested as coolant options (Pickard et al., 2009); however, these are expensive. Packed bed HEX offer potential for high-temperature heat storage with high effectiveness (Barbour et al., 2015; Peng et al., 2016) and would also mitigate some of the losses associated with thermal mixing in the TES; however, large tank sizes with high pressure tolerance may not be cost effective.

Expanders

During discharge, the air expansion process is relatively similar to the operation of closed cycle gas turbines, because the working fluid (air) is externally heated using stored heat from the TES. However, the overall pressure ratio for the expansion is significantly higher than in typical gas turbines for power generation (typical gas turbines have an overall pressure ratio ~10–30) (Sanjay et al., 2007; Horlock, 1995). Therefore, in the conventional CAES systems at Huntorf and MacIntosh, modified steam turbine technology is employed for the high-pressure expansion (Hounslow et al., 1998) and similar customized designs will be required in ACAES. Small-scale experiments have also adapted automotive turbocharge units (Maia et al., 2016); however, poor efficiency (peak instantaneous expansion-only efficiency of 45%) was reported. Although the need for custom design due to the high expansion inlet pressure will increase costs, the temperatures are lower than those encountered in gas turbines—maximum temperatures in modern high-efficiency gas turbines often exceed $1,800K$ (Sanjay et al., 2007) compared with $>600K$ for the design shown in Figure 2. This is favorable from a costs perspective because designing materials to withstand these high temperatures is a significant source of expense in high-efficiency gas turbines and the lower temperatures may increase the power generation ramping rate.

Generally, designing turbines for ACAES is less of a challenge than compressors and HEX. A throttle valve installed upstream of the discharge turbo-machinery can control for a constant pressure ratio, so achieving efficient off-design operation is less critical. Moreover, the overall pressure gradient follows the main flow direction, thus allowing for greater pressure ratios over each expansion stage (compared with the compressors). This way, it is possible to have fewer expansion than compression stages, resulting in cost reduction. However, from a thermodynamic reversibility standpoint it is advantageous to match the compression and expansion paths.

Storage

The simplest and most commonly suggested method of HP air storage consists of an isochoric reservoir, cycling between two set pressure levels as the system charges and discharges. Usually, this role is fulfilled by an underground cavern or artificial steel pressure vessel. Owing to the high pressure involved, the main design challenge is maintaining the necessary structural integrity over long lifetimes at low cost, which favors underground caverns for large-scale systems or smaller artificial stores with low surface-area-to-volume ratios. For underground air storage, the available geology must withstand not only the pressure requirements but also the impact of cyclical temperature fluctuations, potential liquid condensation (a particular challenge in salt-based geology), or any other chemical interactions. The Iowa Stored Energy Park (proposed 270-MW plant with more than $8 million investment) is an example of a project failure due to unsuitable geological conditions. Although appearing suitable at first, low sandstone permeability meant the geology was unable to sustain the required air mass flow (Schulte et al., 2012). Isochoric storage also influences the other components in the system, because the variations in pressure (and mass) in a constant volume mean that the other components must function with variable pressures. This, as discussed already, leads to several design challenges and the air compression within the store also results in thermal mixing (see Figure 3C), although this is generally a small loss.

The alternative to isochoric storage is isobaric storage. By altering the storage volume during the operation, the pressure (and temperature) variation can be mitigated, allowing components to operate at design-point. However, achieving isobaric operation is a major engineering challenge and only a few methods are proposed in the literature. These include sliding, movable barriers (Chen et al., 2018), liquid displacement (Mazloum et al., 2017) from/to an underground cavern to a body of water (e.g., lake), and flexible underwater storage bags (Pimm et al., 2014). Overall, the question for isobaric storage is whether the

Table 2. Major ACAES projects and experimental academic studies

Project	Status	Performance	Documented?	Notes
ALACAES	Underground tunnel air store and TES testing	Simulated 72%	Geissbühler et al. (2018)	The plant does not include a turbine so performance is simulated
ADELE	Project finished, no plant built	Claimed >70%	Zunft et al. (2017)	Planned construction never started due to unfavorable economic conditions
TICC 500	Completed pilot plant	Measured 22.6%	Wang et al. (2016a)	Five-stage reciprocating compressor. Low efficiency ascribed to unsteady operations
Lightsail	Commercial, insolvent	Claimed 90% *thermal efficiency*	No	Raised in excess of $70 million, water injection compression
SustainX	Commercial, insolvent	–	No	Liquid piston compression, US DOE invested $∼ 5.5 million. Pilot plant results never presented
Hydrostor	Commercial, two demonstration plants	–	Partially in Ebrahimi et al. (2019)	Isobaric water displacement storage, first pilot plant uses supplementary electric heater
1.5-MW pilot	Commercial?	Claimed 55%	No	Mentioned in Wang et al. (2017), functional references not provided
10-MW pilot	Commercial?	Claimed >60%	No	Mentioned in Wang et al. (2017), functional references not provided

increase in the performance of other components compensates for the increased complexity in the HP store design.

Performance claims and current state of the technology

Despite two decades of research and significant funding, ACAES remains a technology squarely in early-stage research. To understand why, we review some major experimental studies and the available literature on pilot projects and commercial demonstration plants. These are summarized in Table 2.

We find that most academic studies undertake experiments on individual system components and subsequently use simulation to infer the whole-system performance, rather than experimental analysis on the complete system. For example, Geissbuhler et al. employ a large underground tunnel as an HP air store, testing the pressure integrity of the tunnel and the performance of the TES (Geissbühler et al., 2018). However, their efficiency estimate of 63%–74% is based on simple thermodynamic models of compressors and turbines with constant efficiency across the range of pressures encountered, which is unlikely to be realistic in a real system (Sciacovelli et al., 2017; Wang et al., 2016a). In another notable part-experimental study, sophisticated models of compressors and scroll expanders in small-scale ACAES were developed to fit with measured performance data. An efficiency of 13%–25% for a single-stage ACAES system was estimated, and it was suggested that this could improve to 60% for a 3-stage design (Chen et al., 2020). However, this efficiency relied on a pressure variation less than 0.05*MPa*, with the efficiency dropping rapidly as the pressure variation increased. It must also be noted that the system included no heat exchange—rather the expanding air was reheated to the maximum compression temperature in lieu of heat exchangers and a TES.

Overall, there is precious little published experimental work where work input and output from the system has actually been measured over a full cycle rather than inferred. The European Union-funded project ADELE aimed to build an ACAES plant with 70% efficiency (Zunft et al., 2017); however, no plant was ever built. Despite this, published literature from the project claimed success in confirming 70% efficiency as attainable with existing components (Zunft et al., 2017). The most notable experimental study on a complete ACAES system in the academic literature details a 500-kW ACAES pilot plant, documented in Wang et al. (2016a) and Mei et al. (2015). This plant achieved an electric-to-electric efficiency of 22% (Wang et al.,

2016a), and a major reason for the poor performance was the unsteady operations of compressors and turbines caused by the HP store pressure variation (Wang et al., 2016a). Other studies that have measured work output in small-scale systems have struggled to achieve any reasonable efficiencies. For example, Cheayb et al. built a novel trigenerative CAES system and predicted that favorable efficiencies should be possible; however the measured electrical-to-electrical efficiency was only 3.6% (Cheayb et al., 2019). More often than not, experimental academic studies do not report the cycle efficiency even where this would be possible, instead focusing on metrics like peak instantaneous efficiency, which is defined within a very narrow pressure range.

Outside of the academic studies, there has been significant hype around novel ACAES systems in early-stage commercial ventures, such as Lightsail Energy and SustainX; however, despite promising early press releases—Lightsail made claims of a thermal efficiency around 90% (Chen et al., 2016)—the majority of these companies have ceased trading. Lightsail Energy is a high-profile example of an ACAES startup that raised in excess of $70 million dollars Wesoff (2016) (accessed August, 2020); however, the company has now ceased operations. Despite this, Lightsail is still routinely cited in academic articles without mention that it no longer operates and failed to deploy a prototype. The Canadian venture Hydrostor is an exception that (in 2020) continues to operate with two demonstration ACAES projects and recently won a 2019 Energy Storage North America innovation award. Although technical details about Hydrostor projects are unavailable in the public domain, it is notable that Hydrostor runs an isobaric system using water displacement. This further evidences our suggestion that variable pressure operation is a major challenge for ACAES. Figure 4 provides a timeline of notable demonstration ACAES projects and major experimental publications.

Other demonstration projects have been mentioned in academic reviews with unverified and questionable efficiency claims. A recent CAES review paper cites two of these projects (Wang et al., 2017), mentioning a 1.5-MW demonstration plant with 55% efficiency and a 10-MW demonstration plant with 60% efficiency. However, verification is impossible as the web references provided are no longer available (the domains have expired) and there are no plant locations described in the article (Wang et al., 2017). Given the potential importance of these developments (a novel, large-scale thermo-mechanical energy storage system achieving in excess of 60% round-trip efficiency in a prototype system) this is very surprising. Further discussion of claims made regarding ACAES demonstration plants is available in supplemental information section S2.

DISCUSSION AND RECOMMENDATIONS

The idealized thermodynamic analysis undertaken illustrates some of the limitations of ACAES designs. We find that even with hypothetical, ideal components, 6.4% of the input work may be unrecoverable in a typical design. Although this does not preclude the existence of a successful plant, it highlights limits to the system performance, which have not previously been acknowledged. Furthermore, inspecting the operation required of the components, we find that an ACAES system cannot be built with off-the-shelf components. Additionally, many academic papers are restricted to theoretical and/or numerical assessments that are based on unrealistic assumptions (i.e., constant compressor efficiency and HEX effectiveness), and thus over-predict achievable performance. This over-prediction is compounded by experimental studies, which report metrics such as peak-instantaneous efficiency, rather than measured round-trip efficiency. We suspect that the combination of these factors may have led to over-optimistic development in commercial ventures much too early in the research, development, and demonstration process. Ultimately, despite large amounts of funding, this has led to the failure of most ACAES commercial projects. When further considering the short timeframes for which venture capital or private investors expect a return on investment, it seems likely that ACAES is still unsuitable for commercial development without further significant breakthroughs in the technology.

Isobaric air storage is a promising option for mitigating many of the losses associated with isochoric ACAES. It removes the need for throttling, which is the major limiting factor in idealized systems, and crucially, it allows machinery to operate at design-point. This deviation from design-point operation has been identified by previous studies as a major source of inefficiency (Wang et al., 2016a; Chen et al., 2020). Several isobaric ACAES concepts have been proposed, including underwater air storage (Pimm et al., 2014; Wang et al., 2016b; Cheung et al., 2014), regulating the available storage volume by pumping fluid (Mazloum et al., 2017; Kim et al., 2011), and exploiting the phase change in a volatile fluid (Chen et al., 2018). Although any of these concepts would certainly increase the engineering complexity of the HP store, the difficulties of variable pressure operation make further research on isobaric systems worthwhile.

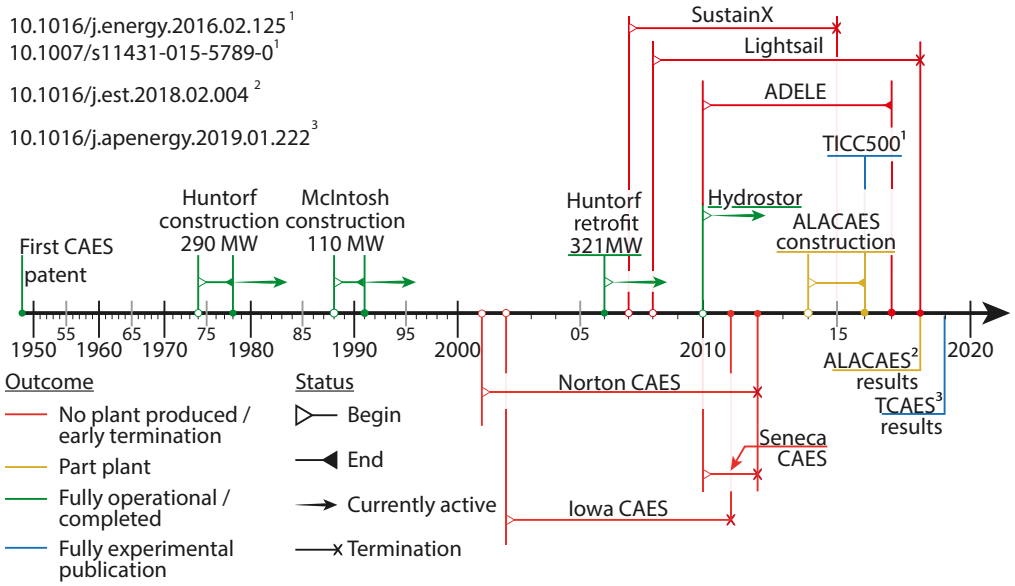

Figure 4. Timeline of major technology milestones

Timeline of CAES/ACAES projects. Blue corresponds to recent prototypes in which energy consumption and generation are directly measured. Yellow are related to the ALACAES publications. Green marks completed or ongoing projects, including Huntorf and MacIntosh. Red shows major failed projects with early termination, bankruptcy, and no physical assemblies.

Future research to improve the performance of the constituent components will also be useful. For compressors, the focus should be on designs with simultaneous high single-stage compression ratios and high isentropic efficiency, with high mass flow reciprocating designs of particular interest. HEX development should focus on increasing contact area in balanced exchangers to minimize irreversibility, and further study of unsteady flow conditions in ACAES heat exchangers needs investigation (Zhang et al., 2019). Future work on systems that use packed beds for one or more of the TES may be promising, as packed beds integrate the heat exchange and thermal storage units and typically have very large contact areas for heat exchange. In particular, they may be well suited for the TES associated with the lower pressure compression stages (Zunft et al., 2017), because packed bed cost increases rapidly at higher pressures (Barbour et al., 2015). Reversible isothermal compression (Weiqing et al., 2020; Zhang et al., 2018) is another interesting avenue for future research, because near-isothermal compression and expansion would remove the need for high temperature TES. This could significantly reduce cost and allow for waste heat integration (Odukomaiya et al., 2016). However, isothermal compressors and expanders are highly experimental and have not been demonstrated at scale.

Finally, we note that history of ACAES is littered with failures and opaque claims of high performance that have subsequently turned out to be untrue. Therefore, we urge caution regarding any performance claims that are presented without clear accompanying evidence. Claims of high performance with no evidence should not be included in academic review articles without explicit mention that they are unverified. Furthermore, press releases on company websites should not be treated as verification, because these have a tendency to pre-claim results in early-stage ventures (to generate hype and investment). Most importantly, unverifiable claims should not interfere with ambitious, transparent, and much-needed experimental work on ACAES systems at universities or other publicly funded institutions. Otherwise there is a danger that *good science* on the subject will be disrupted or go unfunded, hindering progress in the long run. In general, experimental research into the performance of the constituent system components is much needed, especially under the operational conditions anticipated in real grid-scale ACAES systems. There is a particular need to improve the measured performance of heat exchangers and compressors under variable operational conditions and to explore the development of isobaric storage. Academic studies that develop prototype systems should also ensure that they publish the measured round-trip efficiency as well as modeled estimates, so the state-of-the-technology is clearly visible. Where publicly funded research is undertaken by private commercial entities or public-private research partnerships, a minimum level of documentation should be stipulated so that the lessons learned in these projects are available for future

research rather than remaining hidden. In the opinion of the authors, adhering to these recommendations would significantly increase the likelihood of realizing a successful ACAES prototype.

METHODS

Thermodynamics of compression

The work required to compress unit mass flow $\dot{m}$ of air can be estimated by considering a control volume (*CV*) enclosing a compressor at steady state, where the mass flow rates at the inlet and exit of the compressor are equal. The First Law of Thermodynamics yields Equation 6, where u is the specific internal energy (Jkg^{-1}), the flow work pv is the product between pressure p (Pa) and specific volume υ (m^3kg^{-1}), β is the fluid velocity (ms^{-1}), g is the gravitational acceleration (ms^{-2}), and z is the height (m). $\dot{Q}^{CV}$ and $\dot{W}^{CV}$ are the rates of heat added to and mechanical power extracted from the control volume, respectively, given in Watts (W). The superscripts *in* and *out* refer to the control volume inlet and outlet respectively.

$$0 = \frac{\dot{Q}^{CV}}{\dot{m}} - \frac{\dot{W}^{CV}}{\dot{m}} + \left(u^{in} + p^{in}v^{in} + \frac{\beta^{in^2}}{2} + gz^{in}\right) - \left(u^{out} + p^{out}v^{out} + \frac{\beta^{out^2}}{2} + gz^{out}\right) \quad \text{(Equation 6)}$$

We combine the terms u and pv together into specific enthalpy h and neglect the changes in kinetic and potential energies (typically these are much smaller in a compressor or turbine). Furthermore, we assume an adiabatic compression ($\dot{Q}^{CV} \approx 0$) and therefore the work is given by the change in enthalpy from inlet to outlet. Approximating air as a calorically perfect gas (with constant specific heats c_p and c_v) then the enthalpy is only a function of the temperature as shown in Equation 7.

$$-\frac{\dot{W}^{CV}}{\dot{m}} = h^{out} - h^{in} = c_p\left(T^{out} - T^{in}\right) \quad \text{(Equation 7)}$$

For counterflow heat exchangers, the generalized energy balance neglecting thermal losses to the environment and defining an effectiveness ε (the ratio of the actual heat transfer rate to the maximum possible heat transfer $\dot{Q}^{MAX}$) is shown in Equation 8. The minimum heat capacity rate is defined by $C^{MIN} = \text{MIN}[\dot{m}^c c^c, \dot{m}^h c^h]$, where $\dot{m}^c$ and $\dot{m}^h$ are the mass flow rates of the cold/hot fluids, respectively, and c^c and c^h are the cold/hot fluid heat capacities. $T^{h,in}$ and $T^{c,in}$ are the inlet temperatures of the hot and cold fluid, respectively.

$$\varepsilon = \frac{\dot{Q}}{\dot{Q}^{MAX}} = \frac{C^h\left(T^{h,in} - T^{h,out}\right)}{C^{MIN}\left(T^{h,in} - T^{c,in}\right)} = \frac{C^c\left(T^{c,out} - T^{c,in}\right)}{C^{MIN}\left(T^{h,in} - T^{c,in}\right)} \quad \text{(Equation 8)}$$

In reality, the effectiveness is a function of the HEX geometry and fluid properties and can vary greatly within engineering applications (40% in automotive radiators, and in excess of 95% in gas turbine recuperators [Shah and Sekulic, 2003]), and hence will change as the pressure in the store in Figure 2 changes. However, in the limit of perfect heat exchange for balanced counterflow HEX (i.e., $\varepsilon = 1$ and $\dot{m}^c c^c = \dot{m}^h c^h$), the temperature at each compressor inlet will be equal to the ambient temperature T^0, whereas the coolant will leave the HEX at the air inlet temperature. Therefore, we can use Equation 7 to get the incremental work δW^{chg} required to charge the HP air store at pressure p with a mass increment of air δm through N compression stages with equal compression ratio, as shown by Equation 9 and using the fact that the temperature at each compressor outlet is related to the inlet temperature by $T^{out} = T^{in}\left(\frac{p^{out}}{p^{in}}\right)^{\frac{\gamma-1}{N\gamma}}$, where $\gamma = \frac{c_p}{c_v}$ and the superscript ^{0} denotes the ambient state.

$$\delta W^{chg} = N\delta m c_p T^0\left[\left(\frac{p}{p^0}\right)^{\frac{\gamma-1}{N\gamma}} - 1\right] \quad \text{(Equation 9)}$$

For convenience we denote the charging work as the negative of W^{CV}. To relate δm to the storage pressure p, we differentiate the ideal gas law to obtain Equation 10:

$$\frac{dp}{dm} = \left(\frac{\partial p}{\partial m}\right)_T + \left(\frac{\partial p}{\partial T}\right)_m \left(\frac{\partial T}{\partial m}\right)_p. \quad \text{(Equation 10)}$$

The terms $\left(\frac{\partial p}{\partial m}\right)_T$ and $\left(\frac{\partial p}{\partial T}\right)_m$ are easily obtained from the ideal gas law. For the last term, $\left(\frac{\partial T}{\partial m}\right)_p$, we use the conservation of energy for the HP store, expressed by Equation 11:

$$\delta m c_p T^0 + m c_v T = (m + \delta m) c_v (T + \delta T) \quad \text{(Equation 11)}$$

Here m is the air mass already contained within the store, T is the store temperature, and δT is the change in the store temperature due to the addition of air mass δm at temperature T^0. Simplifying this leads to Equation 12.

$$\frac{dT}{dm} = \frac{\gamma T^0 - T}{m} \quad \text{(Equation 12)}$$

Substituting Equations 12 into 10 we find that $\frac{dp}{dm} = \frac{R\gamma T^0}{V^{st}}$. Further substituting this result into Equations 9 leads to 13, which gives the compression work required to raise the HP store pressure p from the initial charge pressure $p^{chg,i}$ to the final pressure $p^{chg,f}$.

$$W^{chg} = \frac{N V^{st} c_p}{R\gamma} \int_{p^{chg,i}}^{p^{chg,f}} \left(\frac{p}{p^0}\right)^{\frac{\gamma-1}{N\gamma}} - 1 \, dp \quad \text{(Equation 13)}$$

Evaluating the integral leads to Equation 1. Assuming the initial storage temperature is the ambient temperature T^0, the final storage temperature is found by integrating Equation 12 and combining with the ideal gas law to give Equation 2.

TES temperature

The TES temperature is given by the coolant temperature at the HEX outlets, which as noted above, is equal to the temperature of the air inlet in the limit of perfect HEX. Hence, the temperature of the TES is constantly changing during charge as the compressor outlet temperatures change. We assume that each TES is perfectly mixed (there is no stratification) and the heat capacity of the thermal fluid is constant. Therefore the mix temperature is the average temperature at the compressor outlet as the store is charged from $p^{chg,i}$ to $p^{chg,f}$, as shown in Equation 14 and once again using $\frac{dp}{dm} = \frac{R\gamma T^0}{V^{st}}$. Evaluating Equations 14 leads to 3.

$$T^{TES} = \frac{\int_0^m T^{out} dm}{\int_0^m dm} = \frac{T^0 \int_{p^{chg,i}}^{p^{chg,f}} \left(\frac{p}{p^0}\right)^{\frac{\gamma-1}{N\gamma}} dp}{\int_{p^{chg,i}}^{p^{chg,f}} dp} \quad \text{(Equation 14)}$$

Thermodynamics of expansion

In Figure 2 we see that the air is throttled to p^{thr} upon leaving the HP store. Therefore, the incremental discharge work (δW^{dis}) available from a mass of air δm expanded through N expansion stages is:

$$\delta W^{dis} = \begin{cases} N \delta m c_p T^{TES} \left(1 - \left(\frac{p^{thr}}{p^0}\right)^{\frac{1-\gamma}{N\gamma}}\right) & \text{if } p \geq p^{thr} \\ N \delta m c_p T^{TES} \left(1 - \left(\frac{p}{p^0}\right)^{\frac{1-\gamma}{N\gamma}}\right) & \text{if } p < p^{thr} \end{cases} \quad \text{(Equation 15)}$$

Applying the conservation of energy to the store during discharge leads to $\frac{dT}{dm} = \frac{T(\gamma-1)}{m}$ and shows the store temperature can be expressed as:

$$T = T^{dis,i} \left(\frac{p}{p^{dis,i}}\right)^{\frac{\gamma-1}{\gamma}} \quad \text{(Equation 16)}$$

where $T^{dis,i}$ and $p^{dis,i}$ are the initial discharge temperature and pressure respectively. Combining this with Equation 10 yields $\frac{dp}{dm} = \frac{R\gamma T}{V^{st}}$, which allows Equation 15 to be expressed with store pressure as the only variable. We further stipulate that the final discharge pressure is equal to the throttle pressure, i.e., $p^{dis,f} = p^{thr}$, which gives the available work as:

$$W^{dis} = N \frac{c_p T^{TES} V}{R\gamma T^{dis,i}} \left[\left(\frac{p^{thr}}{p^0}\right)^{\frac{1-\gamma}{N\gamma}} - 1\right] \int_{p^{thr}}^{p^{dis,i}} \left(\frac{p^{dis,i}}{p}\right)^{\frac{\gamma-1}{\gamma}} dp \quad \text{(Equation 17)}$$

Evaluating the integral in Equations 17 leads to 4.

Limitations of the study

The results of the thermodynamic model developed are limited to a fully ideal, three-stage compression and expansion, isochoric ACAES. However, the detailed description allow for flexibility and adaptability to different conditions and layouts. The results of the present work are intended as a descriptive reference to inherent losses, as well as a generalized calculation procedure. Furthermore, no detailed design procedures for compressors, expanders, and heat exchangers are given, as this is a vast research field that could not fit under the scope of a single publication.

Resource availability

Lead contact

Further information and requests for resources should be directed to the lead contact author Edward R. Barbour, E.R.Barbour@lboro.ac.uk.

Materials availability

This study did not generate new unique reagents or materials.

Data and code availability

All data needed and code developed to draw the conclusions in this paper may be requested from the authors.

SUPPLEMENTAL INFORMATION

Supplemental information can be found online at https://doi.org/10.1016/j.isci.2021.102440.

ACKNOWLEDGMENTS

D.L.P. is supported by a scholarship provided by Loughborough University.

AUTHOR CONTRIBUTIONS

Conceptualiszation, E.R.B.; methodology, E.R.B. and D.L.P.; software, E.R.B. and D.L.P.; validation, E.R.B. and D.L.P.; writing – original draft, E.R.B., D.L.P., and P.E.; writing – review & editing, E.R.B. and D.L.P.; supervision, E.R.B. and P.E.

DECLARATION OF INTERESTS

The authors declare no competing interests.

REFERENCES

Barbour, E., Mignard, D., Ding, Y., and Li, Y. (2015). Adiabatic compressed air energy storage with packed bed thermal energy storage. Appl. Energy *155*, 804–815.

Budt, M., Wolf, D., Span, R., and Yan, J. (2016). A review on compressed air energy storage: Basic principles, past milestones and recent developments. Appl. Energy *170*, 250–268.

Cheayb, M., Gallego, M.M., Tazerout, M., and Poncet, S. (2019). Modelling and experimental validation of a small-scale trigenerative compressed air energy storage system. Appl. Energy *239*, 1371–1384.

Chen, S., Arabkoohsar, A., Zhu, T., and Nielsen, M.P. (2020). Development of a micro-compressed air energy storage system model based on experiments. Energy *197*, 117152.

Chen, L.X., Xie, M.N., Zhao, P.P., Wang, F.X., Hu, P., and Wang, D.X. (2018). A novel isobaric adiabatic compressed air energy storage (IA-CAES) system on the base of volatile fluid. Appl. Energy *210*, 198–210.

Chen, L., Zheng, T., Mei, S., Xue, X., Liu, B., and Lu, Q. (2016). Review and prospect of compressed air energy storage system. J. Mod. Power Syst. Clean Energy *4*, 529–541.

Cheung, B.C., Carriveau, R., and Ting, D.S.-K. (2014). Parameters affecting scalable underwater compressed air energy storage. Appl. Energy *134*, 239–247.

Crotogino, F., Mohmeyer, K.-U. and Scharf, R. (2001), Huntorf CAES: More than 20 years of successful operation, in 'SMRI Spring meeting', Vol. 2001.

Ebrahimi, M., Carriveau, R., Ting, D.S.-K., and McGillis, A. (2019). Conventional and advanced exergy analysis of a grid connected underwater compressed air energy storage facility. Appl. Energy *242*, 1198–1208.

Geissbühler, L., Becattini, V., Zanganeh, G., Zavattoni, S., Barbato, M., Haselbacher, A., and Steinfeld, A. (2018). Pilot-scale demonstration of advanced adiabatic compressed air energy storage, Part 1: plant description and tests with sensible thermal-energy storage. J. Energy Storage *17*, 129–139.

Grazzini, G., and Milazzo, A. (2008). Thermodynamic analysis of CAES/TES systems for renewable energy plants. Renew. Energ. *33*, 1998–2006.

He, W., Luo, X., Evans, D., Busby, J., Garvey, S., Parkes, D., and Wang, J. (2017). Exergy storage of compressed air in cavern and cavern volume estimation of the large-scale compressed air energy storage system. Appl. Energy *208*, 745–757.

Horlock, J. (1995). The optimum pressure ratio for a combined cycle gas turbine plant. Proc. IME Power Energ. *209*, 259–264.

Hounslow, D.R., Grindley, W., Loughlin, R.M., and Daly, J. (1998). The development of a combustion system for a 110 MW CAES plant. J. Eng. Gas Turbine Power *120*, 875–883.

Kim, Y., Shin, D., and Favrat, D. (2011). Operating characteristics of constant-pressure compressed

air energy storage (CAES) system combined with pumped hydro storage based on energy and exergy analysis. Energy *36*, 6220–6233.

Ma, X., Zhang, C., and Li, K. (2019). Hybrid modeling and efficiency analysis of the scroll compressor used in micro compressed air energy storage system. Appl. Therm. Eng. *161*, 114–139.

Maia, T.A., Barros, J.E., Cardoso Filho, B.J., and Porto, M.P. (2016). Experimental performance of a low cost micro-CAES generation system. Appl. Energy *182*, 358–364.

Mason, J.E., and Archer, C.L. (2012). Baseload electricity from wind via compressed air energy storage (CAES). Renew. Sustain. Energy Rev. *16*, 1099–1109.

Mazloum, Y., Sayah, H., and Nemer, M. (2017). Dynamic modeling and simulation of an isobaric adiabatic compressed air energy storage (ia-caes) system. J. Energy Storage *11*, 178–190.

Mei, S., Wang, J., Tian, F., Chen, L., Xue, X., Lu, Q., Zhou, Y., and Zhou, X. (2015). Design and engineering implementation of non-supplementary fired compressed air energy storage system: TICC-500. Sci. China Technol. Sci. *58*, 600–611.

Odukomaiya, A., Abu-Heiba, A., Gluesenkamp, K.R., Abdelaziz, O., Jackson, R.K., Daniel, C., Graham, S., and Momen, A.M. (2016). Thermal analysis of near-isothermal compressed gas energy storage system. Appl. Energy *179*, 948–960.

Peng, H., Yang, Y., Li, R., and Ling, X. (2016). Thermodynamic analysis of an improved adiabatic compressed air energy storage system. Appl. Energy *183*, 1361–1373.

Pickard, W.F., Hansing, N.J., and Shen, A.Q. (2009). Can large-scale advanced-adiabatic compressed air energy storage be justified economically in an age of sustainable energy? J. Renew. Sustain. Energy *1*, 033102.

Pimm, A.J., Garvey, S.D., and de Jong, M. (2014). Design and testing of energy bags for underwater compressed air energy storage. Energy *66*, 496–508.

Raju, M., and Khaitan, S.K. (2012). Modeling and simulation of compressed air storage in caverns: a case study of the Huntorf plant. Appl. Energy *89*, 474–481.

Sanjay, Y., Singh, O., and Prasad, B. (2007). 'Energy and exergy analysis of steam cooled reheat gas–steam combined cycle'. Appl. Therm. Eng. *27*, 2779–2790.

Schulte, R. H., Nicholas Critelli, J., Holst, K. and Huff, G. (2012), Lessons from Iowa: Development of a 270 Megawatt Compressed Air Energy Storage Project in Midwest Independent System Operator, Report SAND2012-0388, Sandia National Laboratories.

Sciacovelli, A., Li, Y., Chen, H., Wu, Y., Wang, J., Garvey, S., and Ding, Y. (2017). 'Dynamic simulation of Adiabatic Compressed Air Energy Storage (A-CAES) plant with integrated thermal storage–Link between components performance and plant performance'. Appl. Energy *185*, 16–28.

Shah, R.K., and Sekulic, D.P. (2003). Fundamentals of Heat Exchanger Design (John Wiley & Sons).

Sun, J., Zuo, Z., Liang, Q., Zhou, X., Guo, W., and Chen, H. (2020). Theoretical and experimental study on effects of Humidity on Centrifugal compressor performance. Appl. Therm. Eng. 115300.

Szablowski, L., Krawczyk, P., Badyda, K., Karellas, S., Kakaras, E., and Bujalski, W. (2017). Energy and exergy analysis of adiabatic compressed air energy storage system. Energy *138*, 12–18.

Wang, J., Lu, K., Ma, L., Wang, J., Dooner, M., Miao, S., Li, J., and Wang, D. (2017). Overview of compressed air energy storage and technology development. Energies *10*, 991.

Wang, S., Zhang, X., Yang, L., Zhou, Y., and Wang, J. (2016a). Experimental study of compressed air energy storage system with thermal energy storage. Energy *103*, 182–191.

Wang, Z., Ting, D.S.-K., Carriveau, R., Xiong, W., and Wang, Z. (2016b). Design and thermodynamic analysis of a multi-level underwater compressed air energy storage system. J. Energy Storage *5*, 203–211.

Weiqing, X., Ziyue, D., Xiaoshuang, W., Maolin, C., Guanwei, J., and Yan, S. (2020). Isothermal piston gas compression for compressed air energy storage. Int. J. Heat Mass Transf. *155*, 119779.

Wesoff, E. (2016). LightSail energy storage and the failure of the founder Narrative. https://www.greentechmedia.com/squared/letter-from-sand-hill-road/lightsail-energy-storage-and-the-failure-of-the-founder-narrative.

Zhang, W., Xue, X., Liu, F., and Mei, S. (2019). Modelling and experimental validation of advanced adiabatic compressed air energy storage with off-design heat exchanger. IET Renew. Power Gener. *14*, 389–398.

Zhang, X., Xu, Y., Zhou, X., Zhang, Y., Li, W., Zuo, Z., Guo, H., Huang, Y., and Chen, H. (2018). A near-isothermal expander for isothermal compressed air energy storage system. Appl. Energy *225*, 955–964.

Zunft, S., Dreissigacker, V., Bieber, M., Banach, A., Klabunde, C. and Warweg, O. (2017), Electricity storage with adiabatic compressed air energy storage: Results of the BMWi-project ADELE-ING, in 'International ETG Congress 2017', VDE, pp. 1–5.

iScience, Volume *24*

Supplemental information

Why is adiabatic compressed air energy storage yet to become a viable energy storage option?

Edward R. Barbour, Daniel L. Pottie, and Philip Eames

S1 Exergy accounting for an ideal isochoric ACAES system - Related to section *Thermodynamic Limits*

S1.1 Charging

The idealised compression work for an N-stage (symmetrical) ACAES system (as shown in Figure 2 in the main text with $N = 3$), assuming the High Pressure (HP) air store is isochoric and adiabatic, with perfect inter-cooling Heat Exchangers (HEX) between the compression stages is given by Equation S1 (also Equation 1 in the main text).

$$W^{chg} = N\frac{V^{st}c_p p_i^{chg}}{R\gamma}\left[\frac{1}{\frac{\gamma-1}{N\gamma}+1}\left(\frac{p_f^{chg}}{p_i^{chg}}\left(\frac{p_f^{chg}}{p^{\emptyset}}\right)^{\frac{\gamma-1}{N\gamma}} - \left(\frac{p_i^{chg}}{p^{\emptyset}}\right)^{\frac{\gamma-1}{N\gamma}}\right) + 1 - \frac{p_f^{chg}}{p_i^{chg}}\right] \tag{S1}$$

This is the minimum input work required for ideal compressors as the store is charged and its pressure p increases from the initial pressure p_i^{chg} to the final pressure p_f^{chg}. Since the store is adiabatic, the temperature also increases from some initial temperature T_i^{chg} to a final temperature T_f^{chg}. The compression work is stored as exergy in the HP store and in the Thermal Energy Stores (TES). In the limit of lossless, balanced, counterflow HEX, the thermal energy added to the TES, by way of a Thermal Fluid (TF), has the same exergy as the air at the compressor outlets (since HEX effectiveness $\varepsilon = 1$ and $\dot{m}^{air}c^{air} = \dot{m}^{TF}c^{TF}$). We can therefore calculate the total exergy in the air added to the HP store and added to the TES.

The incremental exergy added to the HP store with a mass increment δm of air at pressure p is given by Equation S2, where h and s are the specific enthalpy and specific entropy values respectively and $h^{\emptyset}$ and $s^{\emptyset}$ are the enthalpy and entropy at the dead state respectively.

$$\delta B = \delta m\left((h-h^{\emptyset}) - T^{\emptyset}(s-s^{\emptyset})\right) \tag{S2}$$

As the air is an ideal gas and perfect HEX means that it is added to the store at the ambient temperature $T^{\emptyset}$, we can see that $h - h^{\emptyset} = 0$ and the exergy added is due to the change in entropy. This entropy change for an ideal gas is $s - s^{\emptyset} = R\ln(\frac{p}{p^{\emptyset}})$. As described in the Methods section in the main text, we use $\frac{dp}{dm} = \left(\frac{\partial p}{\partial m}\right)_T + \left(\frac{\partial p}{\partial T}\right)_m\left(\frac{\partial T}{\partial m}\right)_p$ and the conservation of energy for the HP air store to find that $\frac{dp}{dm} = \frac{R\gamma T^{\emptyset}}{V^{st}}$. Using Equation S2, this allows us to express the incremental exergy added to the HP store as:

$$\delta B^{HP,add} = \delta p\frac{V^{st}}{\gamma}\ln(\frac{p}{p^{\emptyset}}) \tag{S3}$$

This is integrated to give the exergy added to the HP store as the pressure increases from the minimum pressure p_i^{chg} to the maximum pressure p_f^{chg}, as shown in Equation S4.

$$\begin{aligned} B^{HP,add} &= \frac{V^{st}}{\gamma}\int_{p_i^{chg}}^{p_f^{chg}}\ln\left(\frac{p}{p^{\emptyset}}\right)dp \\ &= \frac{V^{st}}{\gamma}\left[p_f^{chg}\ln\left(\frac{p_f^{chg}}{p^{\emptyset}}\right) - p_f^{chg} - p_i^{chg}\ln\left(\frac{p_i^{chg}}{p^{\emptyset}}\right) + p_i^{chg}\right] \end{aligned} \tag{S4}$$

The incremental exergy added to the each of the N TES is given by Equation S5, where T^{out} is the temperature at each compressor outlet and is given by $T^{in}\left(\frac{p^{out}}{p^{in}}\right)^{\frac{\gamma-1}{N\gamma}}$.

$$\delta B^{TES,add} = \delta m c_p T^{\emptyset}\left(\frac{T^{out}}{T^{\emptyset}} - 1 - \ln\frac{T^{out}}{T^{\emptyset}}\right) \tag{S5}$$

Performing the change of variables from m to p and integrating once again yields the exergy added to the TES as shown in Equation S6. It can be easily verified that the sum of Equations S4 and S6 yields the compression work in Equation S1.

$$\begin{aligned} B^{TES,add} = \frac{NV^{st}c_p}{R\gamma}\Bigg\{ & \frac{1}{[(\gamma-1)/N\gamma]+1}\left[p_f^{chg}\left(\frac{p_f^{chg}}{p^{\emptyset}}\right)^{\frac{\gamma-1}{N\gamma}} - p_i^{chg}\left(\frac{p_i^{chg}}{p^{\emptyset}}\right)^{\frac{\gamma-1}{N\gamma}}\right] - \\ & -p_f^{chg}\ln\left(\frac{p_f^{chg}}{p^{\emptyset}}\right)^{\frac{\gamma-1}{N\gamma}} + p_i^{chg}\ln\left(\frac{p_i^{chg}}{p^{\emptyset}}\right)^{\frac{\gamma-1}{N\gamma}} - \left(\frac{\gamma-1}{N\gamma}-1\right)\left(p_f^{chg}-p_i^{chg}\right)\Bigg\} \end{aligned} \tag{S6}$$

Since the HP air store temperature increases as the pressure rises, there will be some exergy destruction as the air entering the HP store at temperature $T^{\emptyset}$ mixes with the air at variable temperature T in the store. The magnitude of this loss can be calculated by comparing the exergy change in the HP store to the exergy added (Equation S4). This exergy change is given by the final HP store exergy minus the initial store exergy as calculated using the non-flow exergy $B/m = u-u^{\emptyset}+p^{\emptyset}(v-v^{\emptyset})-T^{\emptyset}(s-s^{\emptyset})$, as expressed by Equation S7.

$$\begin{aligned} \Delta B^{HP} = \quad & p_f^{chg}V^{st}\left\{\frac{T^{\emptyset}}{T_f^{chg}}\left[1-\frac{c_v}{R}-\frac{c_p}{R}\ln\left(\frac{T_f^{chg}}{T^{\emptyset}}\right)+\ln\left(\frac{p_f^{chg}}{p^{\emptyset}}\right)\right]+\frac{c_v}{R}-\frac{p^{\emptyset}}{p_f^{chg}}\right\} \quad - \\ & -p_i^{chg}V^{st}\left\{\frac{T^{\emptyset}}{T_i^{chg}}\left[1-\frac{c_v}{R}-\frac{c_p}{R}\ln\left(\frac{T_i^{chg}}{T^{\emptyset}}\right)+\ln\left(\frac{p_i^{chg}}{p^{\emptyset}}\right)\right]+\frac{c_v}{R}-\frac{p^{\emptyset}}{p_i^{chg}}\right\} \end{aligned} \tag{S7}$$

The maximum temperature T_f^{chg} in the HP store can be obtained from the conservation of energy and is given by Equation S8 (Equation 2 in the main text).

$$T_f^{chg} = \frac{\gamma T^{\emptyset}}{\frac{p_i^{chg}}{p_f^{chg}}(\gamma-1)+1} \tag{S8}$$

The exergy destroyed due to mixing in the HP air store can then be directly obtained by subtracting the Equation S7 from Equation S4.

Similarly, exergy is destroyed due to mixing in the TES since the instantaneous compressor outlet temperature depends on the variable store pressure p. To calculate the exergy destroyed due to this temperature mixing, the exergy contained within the TES at the end of the charging period can be compared to the exergy added to the TES as given by Equation S6. The temperature of the TES at the end of the charging period is given by the average temperature at the compressor outlets, shown in Equation S9 (Equation 3 in the main text).

$$
\begin{aligned}
T^{TES} &= \frac{\int_0^m T^{out} dm}{\int_0^m dm} = \frac{T^{\emptyset} \int_{p_i^{chg}}^{p_f^{chg}} \left(\frac{p}{p^{\emptyset}}\right)^{\frac{\gamma-1}{N\gamma}} dp}{\int_{p_i^{chg}}^{p_f^{chg}} dp} \\
&= \frac{T^{\emptyset} p_i^{chg}}{\left(\frac{\gamma-1}{N\gamma}+1\right)\left(p_f^{chg}-p_i^{chg}\right)} \left[\frac{p_f^{chg}}{p_i^{chg}}\left(\frac{p_f^{chg}}{p^{\emptyset}}\right)^{\frac{\gamma-1}{N\gamma}} - \left(\frac{p_i^{chg}}{p^{\emptyset}}\right)^{\frac{\gamma-1}{N\gamma}}\right]
\end{aligned} \tag{S9}
$$

Therefore, the exergy contained in the TES after charging is given by Equation S10, where ΔM^{chg} is the total air mass added to the HP store during the charge.

$$
B^{TES} = \Delta M^{chg} c_p T^{\emptyset} \left(\frac{T^{TES}}{T^{\emptyset}} - 1 - \ln \frac{T^{TES}}{T^{\emptyset}}\right) \tag{S10}
$$

Thus, the exergy destroyed due to mixing in the TES is given by subtracting Equation S10 from Equation S6.

S1.2 Idle period

In the limit that there is no cooling in either the TES or the HP air store, then there will be no exergy loss during the idle period between the charge and the discharge. However, while in real systems the TES is highly insulated and will be designed to minimise thermal losses during the idle period, this is unlikely to be true for the HP air store. Therefore, we consider the effect of cooling which returns the final charging temperature of the HP air store T_f^{chg} to the ambient temperature $T^{\emptyset}$ during the idle period. Since the store is isochoric, the pressure is directly proportional to the temperature and hence the pressure drops from p_f^{chg} to p_i^{dis}, which is the initial discharge pressure given by $p_i^{dis} = p_f^{chg}\left(\frac{T^{\emptyset}}{T_f^{chg}}\right)$. Hence the exergy destroyed as a result of this cooling is given by:

$$
\begin{aligned}
\Delta B^{idle} = p_f^{chg} V^{st} \left\{\frac{T^{\emptyset}}{T_f^{chg}}\left[1 - \frac{c_v}{R} - \frac{c_p}{R}\ln\left(\frac{T_f^{chg}}{T^{\emptyset}}\right) + \ln\left(\frac{p_f^{chg}}{p^0}\right)\right] + \frac{c_v}{R} - \frac{p^0}{p_f^{chg}}\right\} - \\
- p_i^{dis} V^{st}\left[\frac{p^0}{p_i^{dis}} - 1 + \ln\left(\frac{p_i^{dis}}{p^0}\right)\right]
\end{aligned} \tag{S11}
$$

S1.3 Discharging

The air entering the expansion train is throttled to maintain constant pressure, which allows the expanders to operate at close to their design conditions (Sciacovelli et al. 2017, Zhang et al. 2019, He et al. 2017) while the pressure in the store is greater than the throttle pressure, *i.e.* $p \geqslant p^{thr}$. If the expansion is continued with the pressure dropping below the throttle pressure then there will be a constant pressure expansion phase and a variable pressure expansion phase. In this work, we assume that in regular operation the system is designed so that the store pressure is always greater than the throttle pressure (as is the case in both existing diabatic CAES facilities in regular operation - in emergencies the pressure is allowed to reduce below the throttle pressure), hence the discharge work available from perfectly isentropic compressors is given by Equation S12 (Equation 4 in the main text).

$$W^{dis} = N\frac{c_p T^{TES} V^{st}}{RT_i^{dis}}\left[1-\left(\frac{p^{thr}}{p^{\emptyset}}\right)^{\frac{1-\gamma}{N\gamma}}\right]\left[p_i^{dis}-p^{thr}\left(\frac{p^{thr}}{p_i^{dis}}\right)^{\frac{1-\gamma}{\gamma}}\right] \tag{S12}$$

Since the idealised throttling process is isenthalpic, the direct exergy destruction is a result of the change in entropy of the air as it passes through the flow restriction. This direct throttling loss can be calculated by considering the change in the flow exergy of a mass increment of air passing through the throttle valve:

$$\delta B^{thr} = \delta m R T^{\emptyset} \ln\left(\frac{p}{p^{thr}}\right) \tag{S13}$$

The conservation of energy applied to the discharging process yields $\frac{dT}{dm} = \frac{T(\gamma-1)}{m}$, which in turn describes the temperature of the store during the discharge as $T = T_i^{dis}\left(\frac{p}{p_i^{dis}}\right)^{\frac{\gamma-1}{\gamma}}$. The $\frac{dT}{dm}$ term can be combined with $\frac{dp}{dm} = \left(\frac{\partial p}{\partial m}\right)_T + \left(\frac{\partial p}{\partial T}\right)_m \left(\frac{\partial T}{\partial m}\right)_p$, to yield $\frac{dp}{dm} = \frac{R\gamma T}{V^{st}}$, which allows the change of variables from store mass to store pressure in Equation S13. Thus the exergy destruction through the throttle valve during the discharge process to be calculated as:

$$\begin{aligned}\Delta B^{thr} &= \frac{V^{st}T^{\emptyset}}{\gamma T_i^{dis}}\int_{p^{thr}}^{p_i^{dis}}\left(\frac{p_i^{dis}}{p}\right)^{\frac{\gamma-1}{\gamma}}\ln\left(\frac{p}{p^{thr}}\right)dp \\ &= \frac{V^{st}\gamma T^{\emptyset}}{T_i^{dis}}\left[p_i^{dis}\left(\frac{1}{\gamma}\ln\left(\frac{p_i^{dis}}{p^{thr}}\right)-1\right)+p^{thr}\left(\frac{p_i^{dis}}{p^{thr}}\right)^{\frac{\gamma-1}{\gamma}}\right]\end{aligned} \tag{S14}$$

The exergy exhausted from the first heating HEX (HEX4 in Figure 2 in the main text) depends only on the inlet air temperature since we assume that all HEX are balanced and examine the limit where effectiveness $\varepsilon = 1$. Hence the incremental exergy exhausted at the first discharge HEX is given by Equation S15.

$$\delta B^{exh,HEX4} = \delta m c_p T^{\emptyset}\left[\frac{T}{T^{\emptyset}} - 1 - \ln\left(\frac{T}{T^{\emptyset}}\right)\right] \tag{S15}$$

Using the previously developed approach and integrating between the initial and final discharge pressures yields the exergy exhausted from the HEX4 during the discharge:

$$\begin{aligned}B^{exh,HEX4} = \frac{V^{st}c_pT^{\emptyset}}{R\gamma T_i^{dis}}\Bigg\{p_i^{dis}\left(\frac{T_i^{dis}}{T^{\emptyset}} - 2\gamma + \gamma^2 - \gamma\ln\frac{T_i^{dis}}{T^{\emptyset}}\right) - \\ p_f^{dis}\left(\frac{T^{thr}}{T^{\emptyset}} - \left(\frac{p_f^{dis}}{p_i^{dis}}\right)^{\frac{1-\gamma}{\gamma}}\left[2\gamma-\gamma^2+\gamma\ln\left[\frac{T_i^{dis}}{T^{\emptyset}}\left(\frac{p_f^{dis}}{p_i^{dis}}\right)^{\frac{\gamma-1}{\gamma}}\right]\right]\right)\Bigg\}\end{aligned} \tag{S16}$$

For the subsequent HEX (HEX5 and HEX6), the inlet temperature is equal to the previous expander outlet temperature, $T^{out} = T^{TES}\left(\frac{p^{thr}}{p^0}\right)^{\frac{1-\gamma}{N\gamma}}$. Therefore, the incremental exergy exhausted can be expressed as:

$$\delta B^{exh,HEX5} = \delta B^{exh,HEX6} = \delta m c_p T^{\emptyset} \left(\frac{T^{TES}}{T^{\emptyset}} \left(\frac{p^{thr}}{p^{\emptyset}} \right)^{\frac{1-\gamma}{N\gamma}} - 1 - \right. \\ \left. - \ln \left(\frac{T^{TES}}{T^{\emptyset}} \left(\frac{p^{thr}}{p^{\emptyset}} \right)^{\frac{1-\gamma}{N\gamma}} \right) \right) \tag{S17}$$

This is integrated to give Equation S18, which is also equal to the exergy in the exhaust air from the final expander.

$$B^{exh,HEX5} = \frac{V^{st} c_p T^{\emptyset}}{R T^{TES}} \left[\frac{T^{TES}}{T^{0}} \left(\frac{p^{thr}}{p^{\emptyset}} \right)^{\frac{1-\gamma}{N\gamma}} - 1 - \ln \left(\frac{T^{TES}}{T^{\emptyset}} \left(\frac{p^{thr}}{p^{\emptyset}} \right)^{\frac{1-\gamma}{N\gamma}} \right) \right] \\ \times \left(p_i^{dis} - p_f^{dis} \left(\frac{p_i^{dis}}{p_f^{dis}} \right)^{\frac{\gamma-1}{\gamma}} \right) \tag{S18}$$

If the mass of air extracted is less than the mass of air added to the HP store, then some Thermal Fluid (TF) will also remain in the TES units at the TES temperature (T^{TES}), since during the charge we have that $\dot{m}^{air} c_p^{air} = \dot{m}^{TF} c^{TF}$ at all times. The exergy contained in this leftover thermal fluid can be calculated from Equation S19.

$$B^{TES,remain} = N(\Delta M^{chg} - \Delta M^{dis}) c_p T^{\emptyset} \left(\frac{T^{TES}}{T^{\emptyset}} - 1 - \ln \frac{T^{TES}}{T^{\emptyset}} \right) \tag{S19}$$

Finally, the exergy remaining in the HP store is found by comparing the final non-flow exergy of the HP store with the initial exergy at the start of the charge. Equation S20 shows this:

$$B^{remain} = p_f^{dis} V^{st} \left\{ \frac{T^{\emptyset}}{T_f^{dis}} \left[1 - \frac{c_v}{R} - \frac{c_p}{R} \ln \left(\frac{T_f^{dis}}{T^{\emptyset}} \right) + \ln \left(\frac{p_i^{chg}}{p^{\emptyset}} \right) \right] + \frac{c_v}{R} - \frac{p^{\emptyset}}{p_f^{dis}} \right\} \\ - p_i^{chg} V^{st} \left\{ \frac{T^{\emptyset}}{T_i^{chg}} \left[1 - \frac{c_v}{R} - \frac{c_p}{R} \ln \left(\frac{T_i^{chg}}{T^{\emptyset}} \right) + \ln \left(\frac{p_i^{chg}}{p^{\emptyset}} \right) \right] + \frac{c_v}{R} - \frac{p^{\emptyset}}{p_i^{chg}} \right\} \tag{S20}$$

Thus all input and output exergy flows and exergy destruction are accounted for. Table S1 summarises this section.

S2 Current state of ACAES and performance claims - Related to section *Performance claims and current state of the technology*

The purpose of this section is to summarise our understanding of the state of development of major ACAES demonstration projects. We review several projects which include claims about the performance of experimental systems. The EU project ADELE is included since the original stated aim was the construction of an ACAES plant and it is very highly cited in the subject literature.

Exergy component	Calculation reference	Period
Compression work	Equation S1	Charging
Exergy destruction due to mixing in the HP store	Equation S4 − Equation S7	
Exergy destruction due to mixing in the TES	Equation S6 − Equation S10	
Exergy destruction due to HP store cooling	Equation S11	Idle
Direct throttling loss	Equation S14	Discharging
Exhaust exergy from the HEX4	Equation S16	
Exhaust exergy from the HEX5 & 6	$(N-1)\times$ (Equation S18)	
Turbine exhaust exergy	Equation S18	
Exergy remaining in the TES	Equation S19	
Exergy remaining in the HP store	Equation S20	

Table S1: Complete exergy accounting for the idealised ACAES systems presented in the paper.

S2.1 TICC 500 kW pilot plant

Detailed in two papers, Mei et al. (2015) and Wang, Zhang, Yang, Zhou & Wang (2016), this plant has achieved a 23% round trip efficiency (Wang, Zhang, Yang, Zhou & Wang 2016). While the first paper Mei et al. (2015) reports a higher efficiency of 33%, this appears to be a peak instantaneous efficiency inferred over a small portion of the discharge time (see Fig. 9 in Mei et al. (2015)), rather than to be reflective of measured work output over a cycle. The paper states that this efficiency was calculated *"By comparing the consumed power in the compression process and the generated power in the generation process in the same pressure variation range"*. Figure 9 in the paper clearly shows that this version of efficiency is highest when the storage pressure is lowest and the operation is closest to the design condition, highlighting the poor performance of components across a wide pressure range. This is confirmed in Wang, Zhang, Yang, Zhou & Wang (2016), wherein explaining the poor system efficiency the authors reason that *"unsteady operations could result in low efficiency of compression due to the deviation from the designed operations"*.

S2.2 Underground AA-CAES pilot-scale plant Switzerland — ALACAES

Detailed in Geissbühler et al. (2018), this study claims the "*world's first advanced adiabatic compressed air energy storage (AA-CAES) pilot-scale plant*". Actually, the study is primarily concerned with the integrity of the underground storage system which is a tunnel shaped cavern with a volume of $1,942\ m^3$. The TES is also experimentally studied. Estimated round trip efficiencies were presented since the plant neither contained a turbine, nor a suitable compression system (highlighting the lack of off-the-shelf compressors which can be used for ACAES). Instead a conventional air cooled compressor was used and thus the air was heated to $550°C$ (the estimated output temperature of an equivalent purely adiabatic compressor) with an electric heater prior to entering the cavern. The round trip efficiency was estimated in the range 63—74%, however the turbine and compressor models were basic and assumed a constant efficiency across the range of pressure ratios encountered. Hence this cannot be considered as a true demonstration plant, rather a simulation-based estimate augmented with notable experimental work on the cavern and TES. Reported investment in the facility is close to five million US dollars.

S2.3 Project ADELE

This EU funded project is consistently referenced in studies on ACAES, however despite an original mission to build the world's first large-scale ACAES demonstration plant with 70% efficiency and with reports of funding up to €10 million, no plant was ever built. Despite this, the final project documentation claims the *"main achievements include the confirmation of a round-trip efficiency of about 70%"* (Zunft et al. 2017). However, information regarding any technical details of the proposed plant design are scarce, perhaps due to legitimate concerns of commercial sensitivity. Additionally, rather than focus on the system design, a major component of the research focused on the economic case for storage in the German market (Zunft et al. 2017). While this is an important area to research, it is a far cry from building a demonstration plant of a novel thermo-mechanical energy storage system!

S2.4 SustainX

SustainX was a notable commercial isobaric ACAES venture founded in New Hampshire, USA claiming to have developed a highly efficient, near-isothermal ACAES system. Their key concept was to inject a water-air foam into the compression chamber, reducing the temperature rise during the compression and then storing the warm water. The power generation involved reversing this process by re-injecting warm foam and expanding the compressed air. The company received funding from governmental agencies and private investors, promising a rapid technology development in return. Documentation highlighted plans to build a megawatt-scale pilot plant in around three years. In 2012, a Department of Energy (US DoE) report presented the 1.5 MW pilot plant pitch, indicating that the US government invested $\$5,396,023$ in the company along with $\$7,650,565$ coming from private investors, totalling around 13 million dollars (US Department of Energy 2012). There are reports that SustainX raised more than 24 $Mi\,USD$ (Green Tech Media 2015). By August 2013, the DoE published another report, affirming that the company had completed thorough testing on a 40 kW demonstration plant and construction of the 1.5 MW prototype was underway, with the final report publication scheduled to March 2015 (US Department of energy 2013). However, when published, this report only presented preliminary results (US Department of energy 2015). On March 2015, SustainX announced that it would merge with General Compression to create GCX Energy Storage Inc. Despite promises of continuing R&D, GCX has not published any further information regarding the isothermal CAES system and it is notable that an active website is not maintained, strongly indicating that the project has ended. We could not find any scientific papers published regarding the SustainX or GCX work.

S2.5 Lightsail Energy

Founded in 2008, Lightsail Inc. was another notable early-stage commercial venture proposing to develop a near-isothermal compressed air energy storage system. Lightsail generated very significant hype with its founder, Danielle Fong, listed by Forbes magazine in 2012 as one of the world's most influential young entrepreneurs and prominent investors such as Peter Theil and Bill Gates. Lightsail's concept was the injection of water droplets into the compression chamber of a reciprocating compressor, allowing them to reach significant compression ratios with relatively little temperature increase. The warm water spray was then to be re-combined with the pressurised air and the compression processed reversed for the power generation phase. While this is a valid concept on its own, the current water-injected isothermal turbomachinery development stage is still far from commercial viability (Zhang et al. 2018). Reports suggest that Lightsail raised over 70 million dollars, including

several million dollars from the publicly-funded California Energy Commission (Green Tech Media 2016). After 10 years, the company filed for bankruptcy, and once again no significant technological development was achieved (Green Tech Media 2017). As with SustainX, Lightsail has a distinct lack of any reliable information published by dependable scientific sources, rather information is restricted to appearances in regional newspapers and internet forums.

S2.6 Hydrostor

Founded in 2010 in Toronto, Canada, Hydrostor (Hydrostor 2020*b*) is a private near-Isobaric Adiabatic Compressed Air Energy Storage company with two active projects in Canada and one under development in Australia. Their proposed system concept is based on liquid displacement in underwater ACAES systems (Wang, Xiong, Ting, Carriveau & Wang 2016) to prevent significant pressure changes during the operation cycle. As the Hydrostor ACAES charge, air is compressed and thermal energy is then removed and stored. The cool pressurised air is stored in an underwater High-Pressure air store. The inflowing air mass displaces water at near-constant hydrostatic pressure and thus the pressure variation is mitigated. This allows the compressors to run more efficiently, closer to their operational design point. When energy is required, *i.e.,* during peak-demand, air absorbs the thermal energy and is expanded in air turbines. Simultaneously, water reduces the HP store volume maintaining approximately constant pressure (Hydrostor 2020*b*). Hydrostor's first demonstration project was located in Lake Ontario, using six balloon shaped flexible structures to hold air at pressures around 0.55 *MPa* (Ebrahimi et al. 2019). This small R&D concept validation plant has operated since 2015 and is connected to the local power grid.

Hydrostor's second project is a 10 *MWh* ACAES plant in Goderich, Canada which was completed in 2019. Press releases suggest that the plant has a 2.2 *MW* compression system and 1.75 *MW* generation rated power and that the facility is connected to the Independent Electricity System Operator grid system. Its main purpose is to provide peak demand, spinning reserve, peak shaving and power and frequency regulatory services (Hydrostor 2020*b*). The company claims specific power and energy costs of $1,000-3,000\$/kW$ and $150-300\ \$/kWh$. Indications that the plant is operationally successful were published by Hydrostor later in 2019, and the project was granted the 2019 Energy Storage North America innovation award (Hydrostor 2019). Their third project is a proposed 10 *MWh* facility referred to as the "*the Angas ACAES*", located in Strathalbyn, Australia (Hydrostor 2020*a*).

While Hydrostor is success story — given its continuing operation and growing portfolio of plants — there are relatively few details available concerning the technical plant operation. Significant numerical analysis of the Toronto island plant is undertaken in Ebrahimi et al. (2019), suggesting that the storage pressure is around 550 kPa gauge. However, the actual electrical-to-electrical round-trip cycle efficiency of the plant is not stated. Using information from Table 3 in Ebrahimi et al. (2019) that relates to sensors in the real plant, it is clear that the current system efficiency is very poor. This is largely a result of the electric heater which is used to create steam to reheat the air entering the turbine (see Table 3 in Ebrahimi et al. (2019)). It is also notable that the water depth of 55 *m* restricts the operational store pressure to 550 *kPa*, which is likely to result in a relatively low stored energy capacity (the maximum volume of the balloon structures is not given). Very little information is available for the other plants. On September 2019, the company announced a further 37 *mi US*$ funding investment.

S2.7 Other ACAES demonstration projects mentioned in Review papers

There are two very notable plants which have been mentioned in the extensive review paper Wang et al. (2017). These include a ***1.5 MW demonstration project with reported*** 55% ***efficiency*** and a **10 MW demonstration project with reported efficiency in excess of** 60%. While the review paper Wang et al. (2017) implies that both of these plants are operational and the reported efficiencies are measured round-trip cycle efficiency with no supplemental heat addition, it is very difficult to verify these claims since limited other evidence exists in the public domain. The references used in the paper are to commercial websites — a company called Macaoenergy Industry — which are no longer listed as active. Other information regarding the plant is scarce and what we have found is limited to press releases from the China Energy Storage Alliance (China Energy Storage Alliance 2019). While these reiterate the efficiency claims, they are again opaque in terms of providing verification of the plant operation and performance. This is important given the extraordinary global significance of a thermo-mechanical energy storage system achieving an efficiency greater than 60% in a medium-scale pilot plant. On a further anecdotal note, the authors of this study have tried to contact several academics listed as involved with these projects, and while some email responses have been received, no further details have yet been provided.

References

China Energy Storage Alliance (2019), 'Compressed Air Energy Storage: The Path to Innovation', online. Accessed 3 Dec 2020: http://en.cnesa.org/latest-news/2019/9/29/compressed-air-energy-storage-becoming-a-leading-energy-storage-technology.

Ebrahimi, M., Carriveau, R., Ting, D. S.-K. & McGillis, A. (2019), 'Conventional and advanced exergy analysis of a grid connected underwater compressed air energy storage facility', *Applied Energy* **242**, 1198 – 1208.

Geissbühler, L., Becattini, V., Zanganeh, G., Zavattoni, S., Barbato, M., Haselbacher, A. & Steinfeld, A. (2018), 'Pilot-scale demonstration of advanced adiabatic compressed air energy storage, Part 1: Plant description and tests with sensible thermal-energy storage', *Journal of Energy Storage* **17**, 129–139.

Green Tech Media (2015), 'SustainX to Merge With General Compression, Abandon Above-Ground CAES Ambitions', Online. available at: https://www.greentechmedia.com/articles/read/sustainx-to-merge-with-general-compression-abandon-above-ground-caes-ambiti.

Green Tech Media (2016), 'LightSail Energy Storage and the Failure of the Founder Narrative', Online. available at: https://www.greentechmedia.com/squared/letter-from-sand-hill-road/lightsail-energy-storage-and-the-failure-of-the-founder-narrative#gs.n=k=9qI.

Green Tech Media (2017), 'LightSail Energy Enters 'Hibernation' as Quest for Game-Changing Energy Storage Runs Out of Cash', Online. available at: https://www.greentechmedia.com/articles/read/lightsail-energy-cheap-compressed-air-storage-hibernation.

He, W., Luo, X., Evans, D., Busby, J., Garvey, S., Parkes, D. & Wang, J. (2017), 'Exergy storage of compressed air in cavern and cavern volume estimation of the large-scale compressed air energy storage system', *Applied energy* **208**, 745–757.

Hydrostor (2019), 'Hydrostor and NRStor Announce Completion of World's First Commercial Advanced-CAES Facility', Press release. Availavle at : https://www.hydrostor.ca/news-press-1/.

Hydrostor (2020*a*), 'ANGAS A-CAES PROJECT', online. Available at : https://www.hydrostor.ca/angas-a-caes-project/.

Hydrostor (2020*b*), Hydrostor: Advanced Compressed Air Energy Storage, Technical Brochure Rev 2020, Hydrostor. available at: https://www.hydrostor.ca/wp-content/uploads/2020/01/Hydrostor_Brochure_2020.pdf.

Mei, S., Wang, J., Tian, F., Chen, L., Xue, X., Lu, Q., Zhou, Y. & Zhou, X. (2015), 'Design and engineering implementation of non-supplementary fired compressed air energy storage system: Ticc-500', *Science China Technological Sciences* **58**(4), 600–611.

Sciacovelli, A., Li, Y., Chen, H., Wu, Y., Wang, J., Garvey, S. & Ding, Y. (2017), 'Dynamic simulation of Adiabatic Compressed Air Energy Storage (A-CAES) plant with integrated thermal storage–Link between components performance and plant performance', *Applied energy* **185**, 16–28.

US Department of Energy (2012), Isothermal Compressed Air Energy Storage: Demonstrating a modular, market-ready energy storage system that uses compressed air as a storage medium, Tech report, USDoE. Available at: https://www.energy.gov/sites/prod/files/SustainX.pdf.

US Department of energy (2013), SustainX, Inc. Isothermal Compressed Air Energy Storage Fact Sheet, Tech report, USDoE. available at: https://www.energy.gov/sites/prod/files/2015/05/f22/SustainX-Isothermal-Compressed-Air-ES-Aug2013.pdf.

US Department of energy (2015), Demonstration of Isothermal Compressed Air Energy Storage to Support Renewable Energy Production, Tech report, USDoE. available at: https://www.smartgrid.gov/files/documents/Final-Technical-Report-SustainX_DE-OE0000231.pdf.

Wang, J., Lu, K., Ma, L., Wang, J., Dooner, M., Miao, S., Li, J. & Wang, D. (2017), 'Overview of compressed air energy storage and technology development', *Energies* **10**(7), 991.

Wang, S., Zhang, X., Yang, L., Zhou, Y. & Wang, J. (2016), 'Experimental study of compressed air energy storage system with thermal energy storage', *Energy* **103**, 182–191.

Wang, Z., Xiong, W., Ting, D. S.-K., Carriveau, R. & Wang, Z. (2016), 'Conventional and advanced exergy analyses of an underwater compressed air energy storage system', *Applied Energy* **180**, 810 – 822.

Zhang, W., Xue, X., Liu, F. & Mei, S. (2019), 'Modelling and experimental validation of advanced adiabatic compressed air energy storage with off-design heat exchanger', *IET Renewable Power Generation* **14**(3), 389–398.

Zhang, X., Xu, Y., Zhou, X., Zhang, Y., Li, W., Zuo, Z., Guo, H., Huang, Y. & Chen, H. (2018), 'A near-isothermal expander for isothermal compressed air energy storage system', *Applied energy* **225**, 955–964.

Zunft, S., Dreissigacker, V., Bieber, M., Banach, A., Klabunde, C. & Warweg, O. (2017), Electricity storage with adiabatic compressed air energy storage: Results of the BMWi-project ADELE-ING, *in* 'International ETG Congress 2017', VDE, pp. 1–5.